Cellulose (2016) 23:3925–3937
DOI 10.1007/s10570-016-1060-5

ORIGINAL PAPER

Combined effect of carbon nanotubes and polypyrrole on the electrical properties of cellulose-nanopaper

Makara Lay · José Alberto Méndez · M. Àngels Pèlach · Kim Ngun Bun · Fabiola Vilaseca

Received: 16 June 2016 / Accepted: 29 August 2016 / Published online: 19 September 2016

Abstract In the present study, 2,2,6,6,-tetramethylpiperidine-1-oxyl (TEMPO)-oxidized cellulose nanofibers (CNF) were combined with multi-walled carbon nanotubes (MWCNTs) and with hybrid MWCNT/polypyrrole to produce a variety of binary and ternary formulations of conductive nanopapers. By following a simple mixing/sonication/filtering process, a homogeneous and well-distributed CNF-MWCNT nanostructure was formed, resulting in a nanopaper of strong mechanical properties (141 MPa tensile strength and 9.41 GPa Young's modulus) and good electrical conductivity (0.78 S cm^{-1}), for the formulation with 50 wt% of MWCNT. The subsequent in situ polymerization of pyrrole in CNF-MWCNT mixtures produced ternary multiphase CNF-MWCNT-PPy nanopapers with much improved electrical conductivity (2.41 S cm^{-1}) and electrochemical properties (113 F g^{-1} specific capacitance), even using little amounts of MWCNTs. With these materials, improved hybrid capacitors can be designed. The article presents a trend for the application of cellulose nanofibers in the field of green and flexible electronics.

Keywords Conductive nanopaper · Multi-walled carbon nanotube · Polypyrrole · Mechanical properties · Conductivity · Electrochemical properties

M. Lay · J. A. Méndez · M. À. Pèlach · F. Vilaseca (✉)
LEPAMAP Group, Department of Chemical Engineering, Agricultural and Food Technology, Universitat de Girona, 17071 Girona, Spain
e-mail: fabiola.vilaseca@udg.edu

M. Lay · K. N. Bun
Department of Geo-resources and Geotechnical Engineering, Institute of Technology of Cambodia, Russian conf. Blvd, PP Box 86, Phnom Penh, Cambodia

Introduction

Cellulose nanofibers (CNFs) have gained growing interest in the scientific community due to their green, biodegradable and renewable character, and their low density, being used in bionanocomposites for lightweight products (Dufresne 2012). Moreover, CNFs have extremely high mechanical strength due to their high crystallinity, which depends on their preparation and original cellulose sources. For instance, CNF from TEMPO-mediated oxidation has crystallinity degrees between 65 and 95 % (Saito et al. 2007). Their unique properties, in combination with conductive materials, make them a perfect potential candidate for future electronic devices and flexible electronic displays (Yang 2011). Nanocomposites of cellulose nanofibers modified with active porous carbon materials such as carbon nanotubes (CNTs) and graphene are ideal electrode materials for supercapacitors because of their large specific area, which is accessible to the electrolyte, and their high electrical conductivity (Deng et al. 2013).

Carbon nanotubes possess outstanding mechanical properties and their carbon–carbon bonds exhibit high electrical conductivity and thermal stability (Jung et al. 2007), which have the potential to improve the electrical conductivity of CNFs. However, CNTs are intrinsically non-polar whereas CNFs are polar so that they show a poor interface interaction, and carbon nanotubes tend to agglomerate due to the establishment of van der Waals forces. In order to overcome self-aggregation, surface modification of carbon nanotubes is required to improve the dispersion and the interfacial adhesion of CNF-CNT (Ahmed et al. 2013; Salajkova et al. 2013). Several methods for chemical modification of carbon nanotubes, such as covalent, noncovalent (Hirsch 2002), ion adsorption, metal deposition, grafting reaction, and oxidation have been studied to oxidize carbon nanotube materials (Yu et al. 1998). Previous works (Yu et al. 1998; Hung et al. 2008) have suggested that heating in a mixture of concentrated acid oxidants H_2SO_4/HNO_3 in volume ratio of 3:1, carbon nanotubes are very efficiently oxidized and damages to the tubular structure is prevented. In addition, the amorphous carbon and carbon nanoparticles are removed under this oxidation process.

Carbon nanotubes modification was used to reinforce cellulose nanofibers to obtain an electrically conductive nanopaper (Jung et al. 2007) for flexible supercapacitors (Gao et al. 2013). Several attempts have been used to perform CNF-CNT nanocomposites with different methodologies such as electrospinning (Lu and Hsieh 2010) and mixing (Anderson et al. 2010; Adsul et al. 2011; Salajkova et al. 2013). Besides surface modification, good dispersion of CNTs, which depends on pH conditions, is also needed to produce nanocomposites of high strength. Adsul et al. (2011) have studied the effect of pH on the dispersion of CNF-MWCNT. The optimal dispersion was found at pH between 6 and 10 by adding NaOH; the aggregation was observed at pH values below 6 and above 10. However, owing a difficulty for balancing between specific surface area, porosity, strength, and electronic conductivity, as well as the accessibility into internal pores, the specific capacitance of CNT can be moderate, which provides inferior performance for super capacitor applications (Feng 2015).

Among of all newly developed functional materials, CNT/conductive polymers nanohybrid multiphase materials, for instance: CNT/Polyaniline, CNT/PPy and CNT/PEDOT, are playing a key role in high-performance energy storage (Chen et al. 2000; Feng 2015). Moreover, CNT/conducting polymers are even more interesting and promising since they can combine two relatively cheap materials to gain the large pseudocapacitance of the conducting polymers coupled with the conductivity and mechanical strength of the CNTs (Peng et al. 2008). Hybrid structures of carbon nanotubes and conducting polymers were extensively researched with the expectation that the high conductivity and high specific surface area of CNT can greatly enhance the electrochemical capacitor performance of conducting polymers (Yu et al. 2013). Such composites of PPy with CNTs have been reduced the resistance and improved specific capacitance, cycling stability, and energy/power densities of supercapacitor (Nyholm et al. 2011).

In the present work, binary and ternary formulations of conductive nanopapers based on cellulose nanofibrils, multi-walled carbon nanotubes and polypyrrole are produced. The combined effect of carbon nanotubes and a conductive polymer with fast redox reaction is investigated, by looking after nanostructured multiphase cellulose-based materials of good electrical and electrochemical properties. The influence of the chemical composition and the morphology on the mechanical properties, the electrical conductivity and the electrochemical properties is also studied.

Materials and methods

Materials

Bleached Softwood Kraft Pulp from Arauco (Chile) was used as cellulose raw material. Multi-walled carbon nanotubes (MWCNTs) from Sigma Aldrich containing more than 95 % of carbon with an outside diameter and length of 6-9 nm × 5 μm were treated with H_2SO_4/HNO_3 (3:1) reaction mixture prior use. Pyrrole (Aldrich), 98 % of purity, was used for the chemical synthesis of polypyrrole (PPy). Silver paint 3850 was supplied by Holland shielding system BV, Holland. The rest of materials such as $FeCl_3$, tween-80, 2,2,6,6-tetramethyl-1-1-piperidinyloxy (TEMPO), sodium bromide (NaBr), sodium hypochlorite (NaOCl), HCl, NaOH, and NaCl were also supplied

by Sigma Aldrich, and were used without further purification.

Functionalization of multi-walled carbon nanotubes

Multi-walled carbon nanotubes were submitted to surface modification prior use as shown in Scheme 1. Firstly, 0.5 g of MWCNT were mixed with 100 ml of solution of 98 % H_2SO_4 and 65 % HNO_3 (3:1, v/v) by using ultrasonic bath at 80 ± 3°C for 4 h according to previous work (Hung et al. 2008; Wang et al. 2013). MWCNT suspensions were kept cooling before centrifuging for 45 min at 10,000 rpm to remove the remaining solution of H_2SO_4/HNO_3. Later on, a solution of acetone/water (1:1, v/v) was added and centrifuged few times for 30 min and finally centrifuged one more time in distilled water. The precipitated MWCNT was washed with 0.5 M HCl and distilled water subsequently. The filtered product was dried in a vacuum oven 100°C overnight.

Nanopaper preparation

Cellulose nanofibers were prepared by means of TEMPO-mediated oxidation using 10 mmol of NaClO at pH10 with an oxidation reaction time of about 3 h (Fukuzumi et al. 2009). The resulting cellulose suspension was filtered thoroughly with distilled water to remove all non-reacted reagents and free ions. Afterwards, a cellulose suspension at 1 wt% concentration was passed through high-pressure homogenizer (NS1001L PANDA 2 K-GEA) three times at 600 bars of pressure. A transparent CNF gel-like product was obtained and stored at 4 °C before use. Thereafter, the CNF gel was first diluted with distilled water to 0.2 %, and the suspension was dispersed in a sonicator Q700 for 10 min (5 min pulse on, 2 min pulse off, and 5 min pulse on) at 60 % of amplitude. The CNF suspension was filtered overnight using glass filter (HOLDER KIT MILLIPORE) with a nitrocellulose membrane GSWP29325 (hydrophilic membrane) of 0.22 µm pore-size to obtain CNF cake. Nitrocellulose membrane was peeled off, and the obtained cake was put between two pieces of immobile transfer membranes of polyvinilydene fluoride (PVDF) (hydrophobic membrane) of 0.45 µm pore-size before drying in a laboratory sheet dryer. The drying process was done for approximately 20 min at a vacuum pressure of −0.6 bar at 92 ± 3°C (Lay et al. 2016).

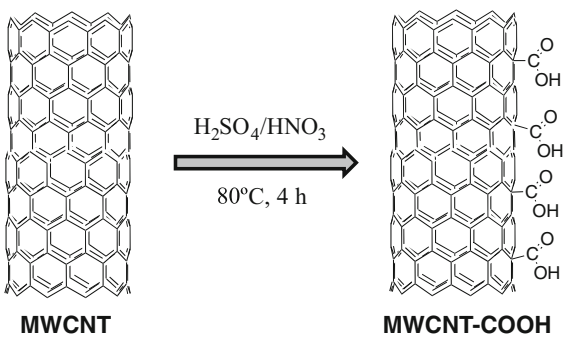

Scheme 1 Functionalization of MWCNT

CNF/MWCNT conductive nanopaper

A combination of mixing/sonication method was used to produce binary CNF-MWCNT and ternary CNF-MWCNT-PPy nanopapers. First of all, the cellulose nanofibers suspension at 0.2 wt% was sonicated for 10 min. MWCNT were dispersed in distilled water (1 mg/mL) using ultra-turrax (IKA, GmbH& Co. KG, Germany) for 3 min. Different amounts of MWCNT (10, 20, 30, 40, and 50 % with respect to CNF content) were added dropwise into the CNF suspension. The CNF-MWCNT mixture was sonicated for 2 min and stirred for 24 h at room temperature to obtain a homogenous distribution of MWCNT in the CNF network. Following similar process for making CNF nanopaper, CNF-MWCNT suspension was filtered overnight using glass filter and dried for 20 min by means of the sheet dryer.

CNF/MWCNT/PPy conductive nanopaper

For the preparation of ternary CNF-MWCNT-PPy nanopaper, the initial mixture of CNF and MWCNT was stirred for 24 h at room temperature. Besides, different amounts of pyrrole monomer (0.1, 0.2, 0.3, and 0.5 ml) were mixed with HCl 0.5 M (1:150 v/v) and stirred for 3 min; one drop of Tween-80 was added into mixture and the magnetic stirring was kept until complete dissolution. Afterwards, the pyrrole-acid solution was added into the CNF-MWCNT suspension and stirred for another 5 min. In order to initiate the polymerization, iron (III) chloride ($FeCl_3$) in HCl 0.5 M was dropwise into the mixture of CNF-

MWCNT, with a molar proportion of 2.4 of $FeCl_3$/pyrrole. After 60 min of reaction time, the suspension was filtered and finally dried for 20 min.

Characterization methods

Elemental analysis

The elemental analysis was made by using a Perkin Elmer EA2400 serie II equipment. The samples were pyrolyzed in helium (He) at a combustion temperature of 925–930°C. Acetanilide powder (C_8H_9NO) was used as reference. The content of carbon, hydrogen, and nitrogen were recorded for 6 min, and the content of PPy in CNF-MWCNT-PPy nanopapers was calculated based on the percentage of nitrogen (N %) (Lay et al. 2016).

Density and porosity

The density was calculated from the basis weight, thickness and dimensions of 1 × 3 cm strips. The porosity was determined from the density of the sample, pure cellulose, MWCNT, and the density of pure polypyrrole and their weight fractions following Eq. 1 (Salajkova et al. 2013).

$$Porosity\,(\%) = 100 \times \left[1 - \frac{\rho_{sample}}{w_{cell} \times \rho_{cell} + w_{MWCNT} \times \rho_{MWCNT} + w_{PPy} \times \rho_{PPy}}\right] \quad (1)$$

where ρ_{sample} is the density of the nanopaper and ρ_{cell}, ρ_{MWCNT}, and ρ_{PPy} are the density of CNF, MWCNT, and PPy, assumed to be 1.5 g cm^{-3} (Henriksson et al. 2011), 2.1 g cm^{-3} (Salajkova et al. 2013), and 1.48 g cm^{-3} (Saville 2005), respectively. The respective weight fractions are represented by W_{cell}, W_{MWCNT}, and W_{PPy}.

Fourier transform infrared spectroscopy (FT-IR)

The chemical compositions of CNF, PPy, MWCNT-COOH, CNF-MWCNT, and CNF-MWCNT-PPy nanopapers were characterized by FT-IR from Bruker with a PLATINUM-ART under transmittance mode in range between 500 and 4000 cm^{-1} using 24 scans at resolution of 4 cm^{-1}.

Field emission scanning electron microscopy (FE-SEM)

The cross section surfaces of cellulose nanofibers (CNF), CNF-MWCNT, and CNF-MWCNT-PPy nanopapers, as well as of the modified-MWCNT, were observed by FE-SEM (HITACHI S-4100). The samples were gold coated using a sputter (EMITECH K550). The images were taken using secondary electron detector at different accelerating voltage MWCNT (20 kV), CNF (12 kV), and at the lower voltage of 5 kV for both CNF-MWCNT and CNF-MWCNT-PPy nanopapers to prevent burning the samples during observation.

Tensile properties

Mechanical properties (tensile strength, Young's modulus and strain at break) of all samples were evaluated using a Universal Testing Machine HOUNSFIELD, equipped with a 250 N load cell with a crosshead speed of 5 mm/min. Specimens were cut in rectangular shape of (50 × 5 × (0.060 ± 0.010)) mm and kept under controlled condition of 50 % relative humidity at room temperature. These parameters were set according to previous work (Hamedi et al. 2014). At least five specimens from each formulation were tested for statistical purpose.

Electrical conductivity

In order to measure the electrical conductivity, the samples were cut into (5 × 20 × (0.06 ± 0.01)) mm stripes. Silver paint was applied at the end of both sides of each sample and kept 16 h at room temperature to ensure good electrical contact with the clip probes (Nyström et al. 2012). Agilent 34461A digital multimeter was used to measure the resistance (R) over the length of the stripes of the specimens. The conductivity was calculated from Eq. 2, where σ, L, w, and d are conductivity, length, width, and thickness of the sample, respectively. R is the resistance (Ω) measured from the multimeter (Lay et al. 2016).

$$\sigma = L/(R \times w \times d) \quad (2)$$

Cyclic voltammetry (CV)

A Potentiostat/Gavanostat Model 273A Princeton with a three-electrode electrochemical system consisting of the sample as working electrode, a platinum wire as counter electrode, and a 2 M NaCl-saturated Ag/AgCl electrode as reference electrode was used for the electrochemical measurement of the conductive nanopapers. The data were recorded in the potential window of −0.9 to +0.9 V vs Ag/AgCl with different scan rate from 5 to 200 mV s^{-1}. The CView and originPro software were used to plot cyclic voltammogram, and the specific capacitance was obtained following by Eq. 3 (Yang et al. 2015):

$$C_{sp} = i/(m.v.\Delta V) \quad (3)$$

where C_{sp} (F g^{-1}) is the specific capacitance, i is the integration in CV curve, which was calculated from originPro, v is the scan rate in V s^{-1}, and m is the mass (g) of electrode material, $\Delta V = 1.8$ V (potential window).

Results and discussion

The three different types of nanopapers prepared in this work, CNF, CNF-MWCNT, and CNF-MWCNT-PPy, are shown in Scheme 2. The produced CNF nanopaper (55 μm of thickness) was highly transparent, while CNF-MWCNT and CNF-MWCNT-PPy nanopapers were black and opaque. All nanopapers were very smooth, flexible and foldable.

The pristine MWCNTs (Fig. 1a (1)) agglomerated and precipitated immediately after dispersion in water, resulting in a poor combination with CNF matrix after 1 week (Fig. 1b (3)) and even worst after one month (Fig. 1c (3)). In contrast, Fig. 1a (2) and Fig. 1a (4) demonstrates a homogenous and stable suspension of acid treated-MWCNT (1 mg/mL) in distilled water and in CNF, respectively. These solutions were stable after one month (Fig. 1c). Figure 1d illustrates the transmittance FTIR spectra of pristine and modified MWCNT. Several peaks appearing in the spectrum of

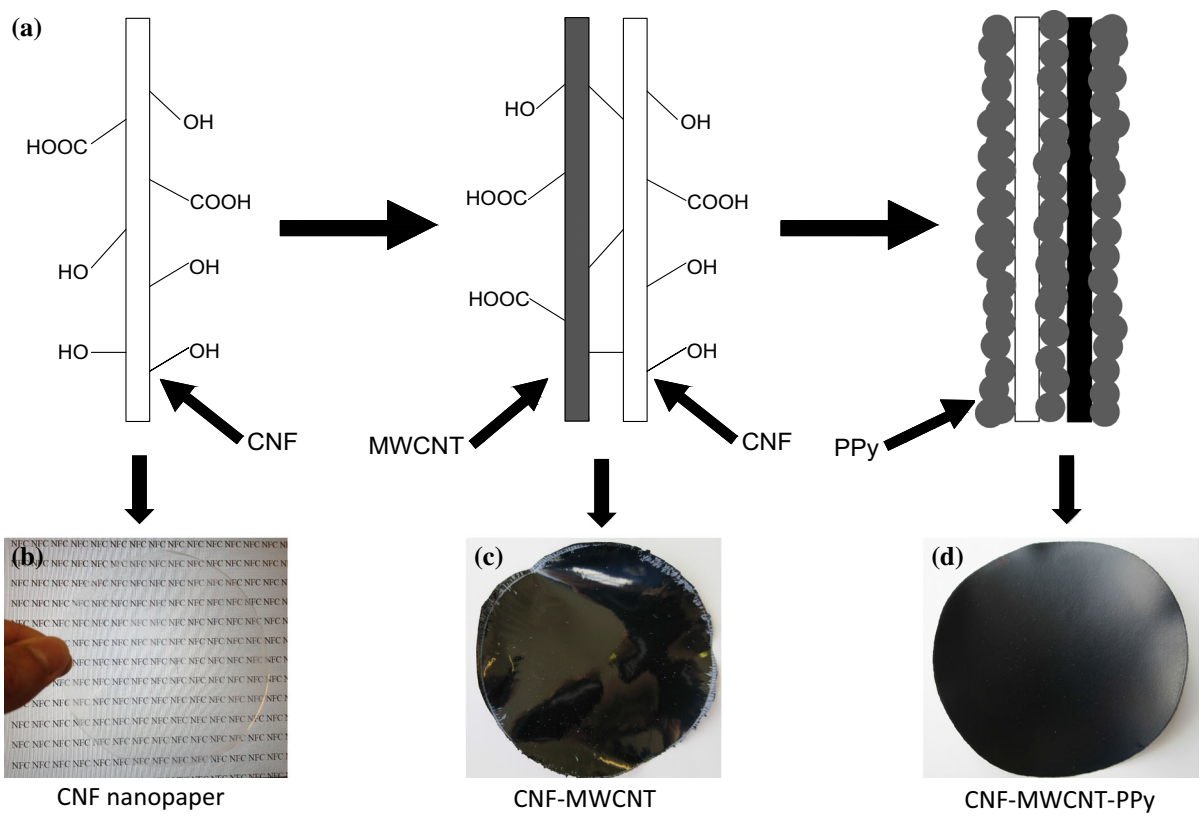

Scheme 2 **a** Illustration for the interaction between TEMPO-oxidized CNF and MWCNTs and further coating with PPy; and **b**–**d** pictures of CNF, CNF-MWCNT and CNF-MWCNT-PPy nanopapers

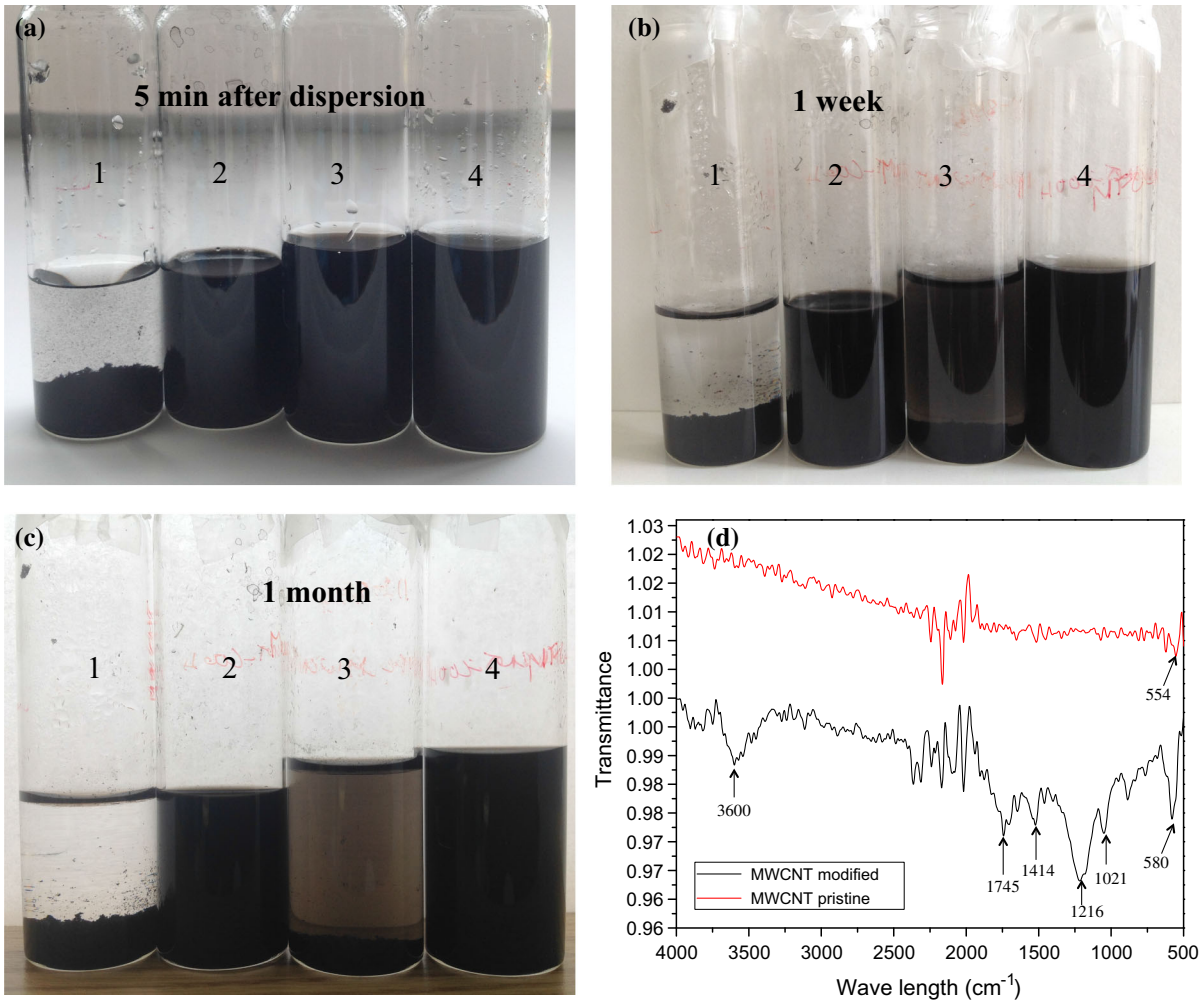

Fig. 1 **a** Pictures of suspensions 5 min after sonication, **b** one week after sonication, and **c** one month after sonication for (1) pristine MWCNT in distilled water, (2) modified MWCNT in distilled water, (3) MWCNT in CNF suspension and (4) modified-MWCNT in CNF suspension; **d** FT-IR of pristine and surface modified-MWCNT

modified-MWCNTs supported the oxidation of MWCNT by the acid treatment. The formation of O–H bonds of alcohol groups is shown by the peak centred at 3600 cm^{-1}. The absorption band at 1745 cm^{-1} is ascribed to C=O stretching and the peak at 1414 cm^{-1} is associated to the bending deformation of O–H in carboxylic acid groups. The C–O stretching and the ether C–O–C functionalities in the modified-MWCNTs were found in the region of 1216 and 1021 cm^{-1}, respectively. These results support the schematic representation of the acid treatment of MWCNT, which consist of the surface oxidation to form carboxylic and hydroxyl groups on MWCNT surface, in good agreement with previous work (Goyanes et al. 2007).

The spectra of cellulose nanofibers (CNF), Polypyrrole (PPy), CNF-MWCNT, and CNF-MWCNT-PPy nanopapers are provided in Fig. 2. The spectrum of CNF (Fig. 2a) exhibits the vibration of –OH groups and C–H stretching of cellulose at the wide bands of 3340 and 2898 cm^{-1}, respectively (Kargarzadeh et al. 2012). A prominent sharp peak at 1602 cm^{-1} is attributed to the stretching of carbonyl group of TEMPO oxidized CNF (Soni et al. 2015). The symmetric bending of CH_2 and C–O groups of the pyranose ring of CNF are found respectively at 1416

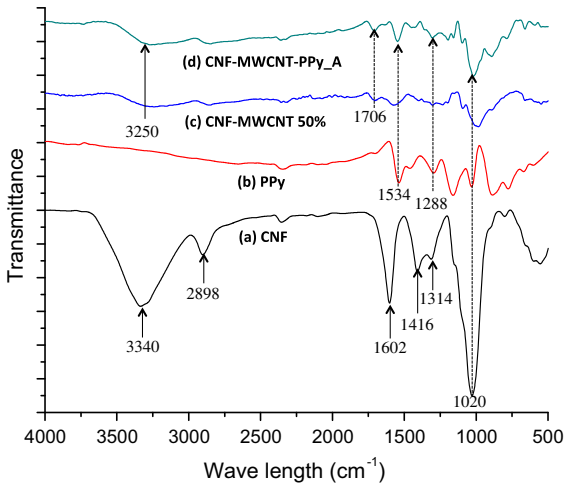

Fig. 2 FT-IR spectra of (*a*) CNF, (*b*) PPy, (*c*) CNF-MWCNT50, and (*d*) CNF-MWCNT-PPy_A

and 1314 cm^{-1} (Kargarzadeh et al. 2012). In the range of 1203 and 1157 cm^{-1} showed symmetrical and asymmetrical stretching (C–O–C). The peak observed at 1024 cm^{-1} due to the C–O stretch in ether groups. Moreover, C–H out-of-plane bending of CNF is found at the region around of 605 cm^{-1}. The bands of neat PPy are clearly observed in Fig. 2b. The absorption band at 1534 cm^{-1} shows the characteristic of C=C stretching of the aromatic ring, and the peak at 1449 cm^{-1} is assigned to the stretching vibration of C–C and C–N links. The absorption peak at 1288 cm^{-1} is assigned to a mixed bending and stretching vibration associated to the C–N bond of the aromatic amine. At this wavelength, single C–C bonds between rings also appear; however its intensity is much lower compared to the C–N bond that has greater dipole (Saville 2005). The C–H in-plane and out-of-plane bending deformation of PPy appears at 1160 and 1036 cm^{-1}, respectively. Also centred at 1160 cm^{-1}, the stretching for the C=N link is found. Finally, the peak at 853 cm^{-1} is related to the N–H wagging of secondary amines (Lay et al. 2016). The spectrum in Fig. 2c corresponds to CNF nanopaper containing 50 % of MWCNT. The absorption peaks at 1706, 1421, and 1017 cm^{-1}, are assigned to C=O, O–H, and C–O of carboxylic acid of MWCNT. Moreover, the change in intensity of the peak at 3250 cm^{-1} may be due to the formation of intermolecular hydrogen bonds between modified nanotubes and cellulose.

The good dispersion of modified nanotubes with nanocellulose may be due to the disruption of intramolecular hydrogen bonds in the cellulose (3340 cm^{-1}, Fig. 2a) by hydroxyl groups (3600 cm^{-1} in Fig. 1d) present on the nanotube surface and by the creation of intermolecular hydrogen bonds (3250 cm^{-1}, Fig. 2c) (Adsul et al. 2011). The spectrum of CNF-MWCNT-PPy (Fig. 2d) contains the same peaks corresponding to CNF-MWCNT, together with the peaks at 1526, 1285, 1149, 970, and 760 cm^{-1}, identified above as functional groups of PPy, confirming the presence of PPy in the sample.

The microstructure of surface modified MWCNTs (Fig. 3a) shows fragments and defects, and some nanotubes shortened in length after the acid treatment process, which produced carboxylic units, and also carbonyl and hydroxyl groups at MWCNT surface. PPy platelets with diameter of between 50 and 150 nm appear aggregated together as illustrated in Fig. 3b. CNF nanopaper (Fig. 3c) exhibited a compact multi-layer configuration with layers of cellulose nanofibers interconnected that will result in high mechanical performance of CNF nanopaper.

The dispersion with 10 % MWCNTs in CNF matrix leads to less dense structure compared with when the amount of MWCNTs was increased up to 50 % (Fig. 3d, e, respectively), probably due to the less strong interaction between nanocelluloses and nanotubes (Salajkova et al. 2013). Moreover, the coating of PPy on CNF and MWCNT (Fig. 3f) resulted in a rougher and less compact CNF-MWCNT-PPy nanopaper. This can be explained due to the intrinsically weaker PPy–PPy interactions with respect to those of cellulose-nanotube, nanotube–nanotube or cellulose–cellulose connections (Pandey et al. 2015).

The stress–strain curves in uniaxial tension, the ultimate tensile strength and Young's modulus of CNF, CNF-MWCNT, and CNF-MWCNT-PPy are presented in Fig. 4. Additional data such as sample composition, density, porosity, and the electrical conductivity are provided in Table 1. Stress–strain curves (Fig. 4a) reveal a linear elastic behaviour at a low strain (<0.7 %) corresponding to Young's modulus. At a stress in the region of 100–130 MPa there is a knee in the stress–strain curve, corresponding to the apparent yield stress, followed by a linear and strongly strain-hardening plastic region. Compared to previous works (Sehaqui et al. 2011; Salajkova et al. 2013; González et al. 2014), our CNF nanopaper exhibited

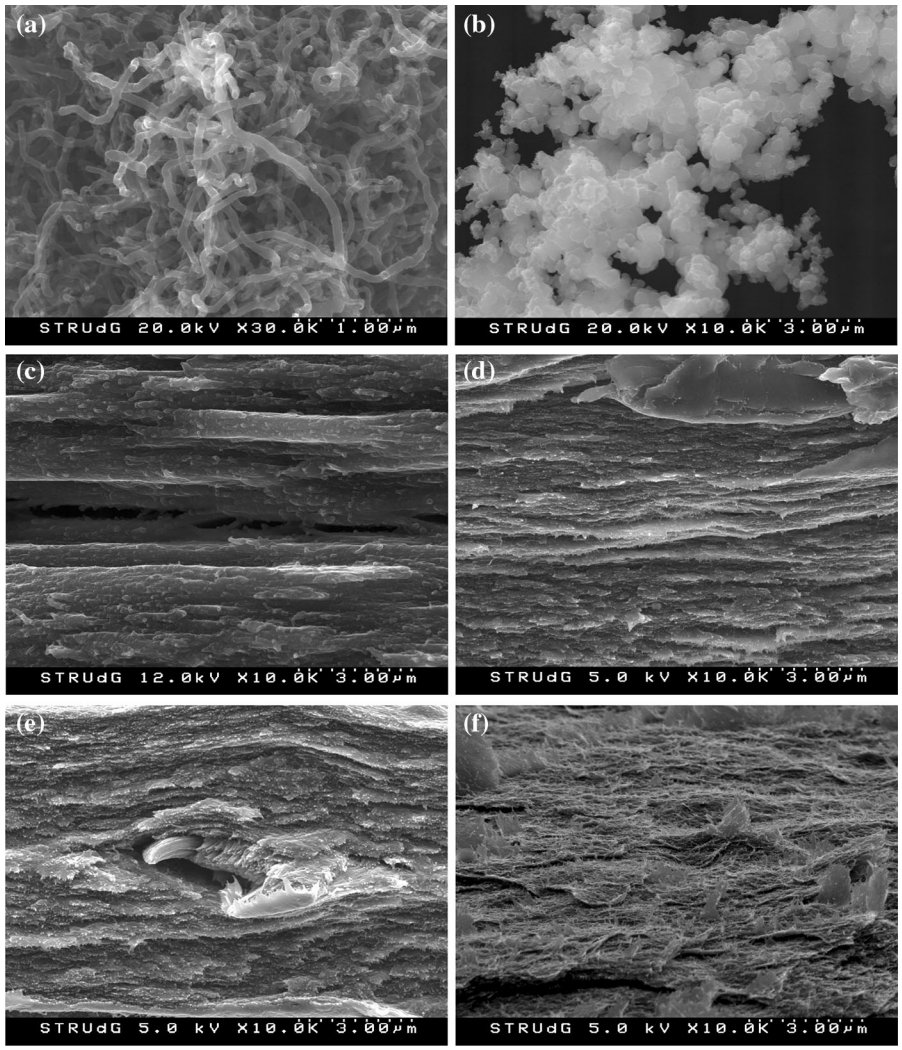

Fig. 3 SEM microphotographs of **a** MWCNTs, **b** PPy, and cross section of **c** CNF, **d** CNF-MWCNT10, **e** CNF-MWCNT50, and **f** CNF-MWCNT-PPy_A nanopapers

outstanding mechanical behaviour, with tensile strength of 224 MPa, Young's modulus of 14.5 GPa and elongation at break of 5.6 %. The strong interactions between fibrils, good fibrils alignment, and nanofibrils entanglements are the reasons of this mechanical behaviour. The negatively charged nanofibres from TEMPO oxidation formed a strong and tough nanopaper. The mechanical performance was weakened with the addition of MWCNTs. For instance, the tensile strength and Young's modulus decreased around 30 and 38 %, respectively for CNF-MWCNT10 nanopaper. With the incorporation of up to 30wt% of MWCNTs, the tensile strength continued to decrease around 130 % for CNF-MWCNT30 nanopaper, whilst the Young's modulus was maintained with the incorporation of the same amount of MWCNTs. The increase in porosity and the lower interaction between CNF and MWCNTs explain the effect on the mechanical properties of nanopapers. The negative charges of carboxylic acid groups in TEMPO oxidized CNF and in modified MWCNTs are the reason for the electrostatic repulsion between them, increasing the porosity of the nanopapers (Table 1). MWCNTs behave as foreign component, and the acid treatment under ultrasonication also provokes defects and breakages of MWCNTs that diminished their

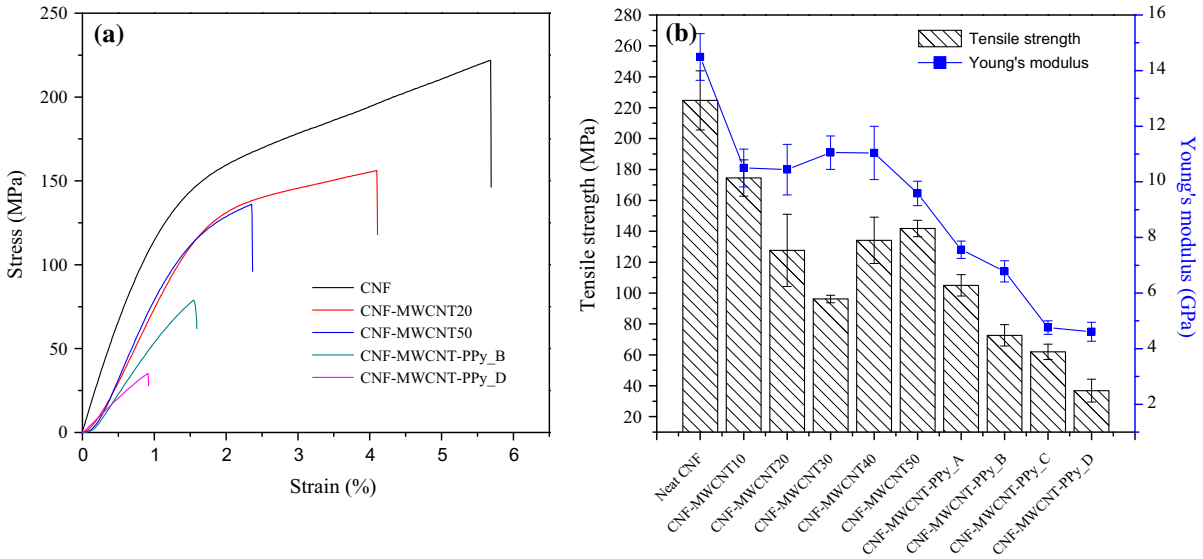

Fig. 4 Stress–strain curves and **b** Ultimate tensile strength and Young's modulus of CNF, PPy, and CNF/PPy nanopapers

Table 1 Composition, density, porosity, tensile strength, Young's modulus, and electrical conductivity of nanopapers

Samples	CNF (%)	MWCNT (%)	PPy (%)	Density (g cm^{-3})	Porosity (%)	Tensile strength (MPa)	Young's modulus (GPa)	Conduc-tivity (S cm^{-1})
Neat CNF	100	0	–	1.27	15.34	224±19	14.49±0.84	
CNF-MWCNT10	90	10	–	1.30	16.35	174±11	10.49±0.68	0.0002
CNF-MWCNT20	80	20	–	1.33	18.04	127±23	10.44±0.91	0.0235
CNF-MWCNT30	70	30	–	1.36	19.09	96±02	11.05±0.60	0.2629
CNF-MWCNT40	60	40	–	1.37	20.99	134±14	11.04±0.96	0.4408
CNF-MWCNT50	50	50	–	1.44	20.21	141±05	9.57±0.43	0.7823
CNF-MWCNT-PPy_A	70	10	20	1.25	19.08	105±07	7.55±0.30	0.0480
CNF-MWCNT-PPy_B	60	9	31	1.18	23.07	72±06	6.78±0.37	0.4250
CNF-MWCNT-PPy_C	52	8	40	1.12	26.72	58±05	4.61±0.24	1.4370
CNF-MWCNT-PPy_D	45	7	48	1.06	29.81	36±07	4.60±0.34	2.4133

intrinsic mechanical properties. Claiming successful preparation, controlling the microstructure of such nanocomposites system remains a challenge due to the strong interaction forces that cause the formations of bundles and clusters, as well as the dispersion and arrangement of MWCNTs in the matrix (Yan Huang and Terentjev 2012). With the addition of higher amounts of MWCNTs, however, the tensile strength started to increase 32 % compared to CNF-MWCNT30. This could be a result from sufficient nanofiller–nanofiller interaction for favourable stress-transfer, which leads to strong matrix-nanofiller interface. It is important to notice that nanopapers maintain very good mechanical properties even at 50 % of MWCNTs. The strain at which the yield occurs decreases with increasing MWCNT content. It is noteworthy to mention, however, that the stress–strain behaviour of our nanopapers with high MWCNT content (20–50 wt%) is interestingly superior than that of other MWCNT nanopapers from previous study (Salajkova et al. 2013), where with only a 16 wt% of MWCNT the ultimate stress and elastic modulus was significantly reduced. Instead, a dramatic decreased of the mechanical behaviour was observed after coating with polypyrrole, for CNF-MWCNT-PPy nanopapers. The weak mechanical properties is the drawback for

the combination of MWCNT and conducting polymers (Baughman et al. 2002). The result reveals that tensile strength decreased 4.8 times and Young's modulus decreased 2.3 times, with respect to the CNF-MWCNT10 nanopaper. Moreover, they became more fragile than CNF-MWCNT nanopapers, confirmed by the diminishing of the elongation at break (Fig. 4a). The addition of PPy conductive polymer gave more porous nanopapers, which can reduce capillarity effects during drying. CNF nanofibrils interact less during drying, due to the presence of MWCNT and PPy, and the porosity becomes higher. It must be emphasized that the material kept its flexibility and foldability with the addition of either 50 % of MWCNT or 48 % of PPy.

The presence of MWCNT in CNF changed the electrical properties of nanopapers (Table 1). When 10 % of MWCNTs were added, good electrical conductivity was obtained indicating that the MWCNTs were uniformly incorporated into the cellulose nanofibers network. The conductivity of nanopaper with 50 % of MWCNT reached 0.7823 S cm^{-1} because the MWCNTs within the CNFs network created a conductive pathway. However, this value is still low considering the electrical conductivity of pristine MWCNT that is in the range of the metallic materials. One reason for this is the acid surface modification of MWCNT, where defects on MWCNT sidewall occurred by forming carboxylic and other oxygen-containing groups on their surface, reducing the electronic conductivity of MWCNT (Li and Zhitomirsky 2013). One more aspect to consider is that carbon nanotubes, which consist of negative charges of carboxylic, leaded to increased porosity of nanopapers as shown in previous works (Salajkova et al. 2013).

Formulations containing PPy showed a significant improvement in the electrical conductivity as shown in Table 1. In CNF-MWCNT-PPy_B nanopaper, with only 9 % of MWCNT and by adding 31 % of PPy, the conductivity was similar to that of nanopapers with 40 wt% of MWCNT. Moreover, the conductivity increased with the PPy content; PPy chains build a good conductive network by wrapping around both cellulose nanofibrils and MWNTs, which favoured the electron transport through the sample.

Conductive filler networks that follow classical geometrical percolation theory (where filler bonding occurs) obey a universal conductivity-loading relationship above the percolation threshold (Hermant 2009), according to the following Eq. 4:

$$\sigma \propto (\Phi - \Phi_c)^t \tag{4}$$

where σ is the conductivity, Φ the volume fraction of the conductive filler and Φ_c the percolation threshold. In this theory, the conductivity increases sharply with increasing the volume fraction of the conductive fillers. To determine the percolation threshold (Φ_c experimental results were fitted by plotting log σ versus log $\Phi-\Phi_c$, and the value of Φ_c was incrementally varied until the best linear fit was obtained. Depending on the matrix, the processing technique, and the type of conductive filler, percolation thresholds has been reported in the range from 0.001 wt% to more than 10 wt% (Koga et al. 2013). In our case, the percolation thresholds of MWCNT and MWCNT-PPy in nanopapers were found to be 0.06 and 0.2 respectively. For each value of Φ_c, the exponent t has been determined from the slope of the linear relation of log σ and log $\Phi-\Phi_c$. For formulations (CNF-MWCNT and CNF-MWCNT-PPy nanopapers), the experimental conductivity and their predicted values with respect to the volume fraction are presented in Fig. 5. The linear correlation between log σ and log $\Phi-\Phi_c$ is presented in Fig. 5b. In the current case, the critical exponents t were found to be 2.62 and 2.76, for the binary and ternary formulations respectively. Many conductive filler networks, including carbon

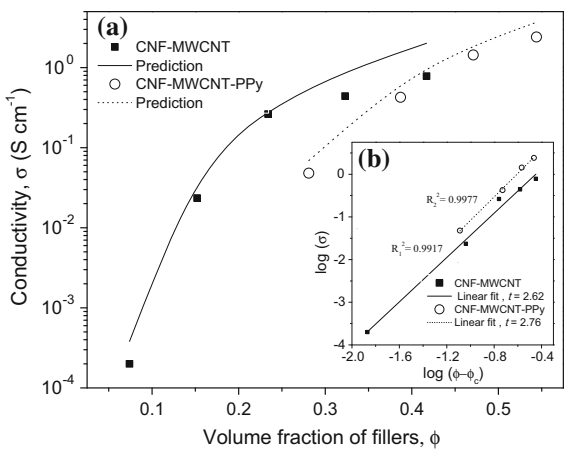

Fig. 5 **a** Experimental and predicted electrical conductivities of CNF-MWCNT (*square*) and CNF-MWCNT-PPy (*circle*) nanopapers with the volume fraction of conductive fillers and **b** Linear correlation between log σ and log $\Phi-\Phi_c$ and predicted t values for 4

nanotube in polymeric composites, exhibit a non-universal value for *t*. This has been linked to the fact that the electrical percolation networks in these systems are not geometrical and tunnelling between nearest-neighbours governs the conduction mechanism.

The specific capacitance results from cyclic voltammetry are plotted in Fig. 6. In all samples, the specific capacitance decreased with increasing the scan rate. The specific capacitances of CNF-MWCNT20 and CNF-MWCNT50 at 5 mv s^{-1} were 1.38 and 16.4 F g^{-1}, respectively. Carbon nanotubes can be employed as high energy density electrode materials because of their good conductivity, however, as a consequence of the lack of micropores for ions accumulation, it is difficult to obtain a high capacitance over a pure carbon nanotube based electrode (Xiong et al. 2015). Zhang et al. (2009) explained that although MWCNTs has high specific surface area (>1000 m^2/g), the specific capacitance is usually smaller than 100 F g^{-1} because not all of the internal surface, such as those of the wall of micro-pores, can be accessed by ions in the activated carbon for charge storage. Peng et al. (2007) also found that the untreated CNTs had a specific capacitance about 10 F g^{-1}, and this property improved five times after acid treatment (50 F g^{-1}). The surface modified MWCNTs helped to improve the specific capacitance. The ternary formulation with 48 % of PPy content had a capacitance of 113 F g^{-1}, around seven times higher than the one of binary formulation with 50 % MWCNT.

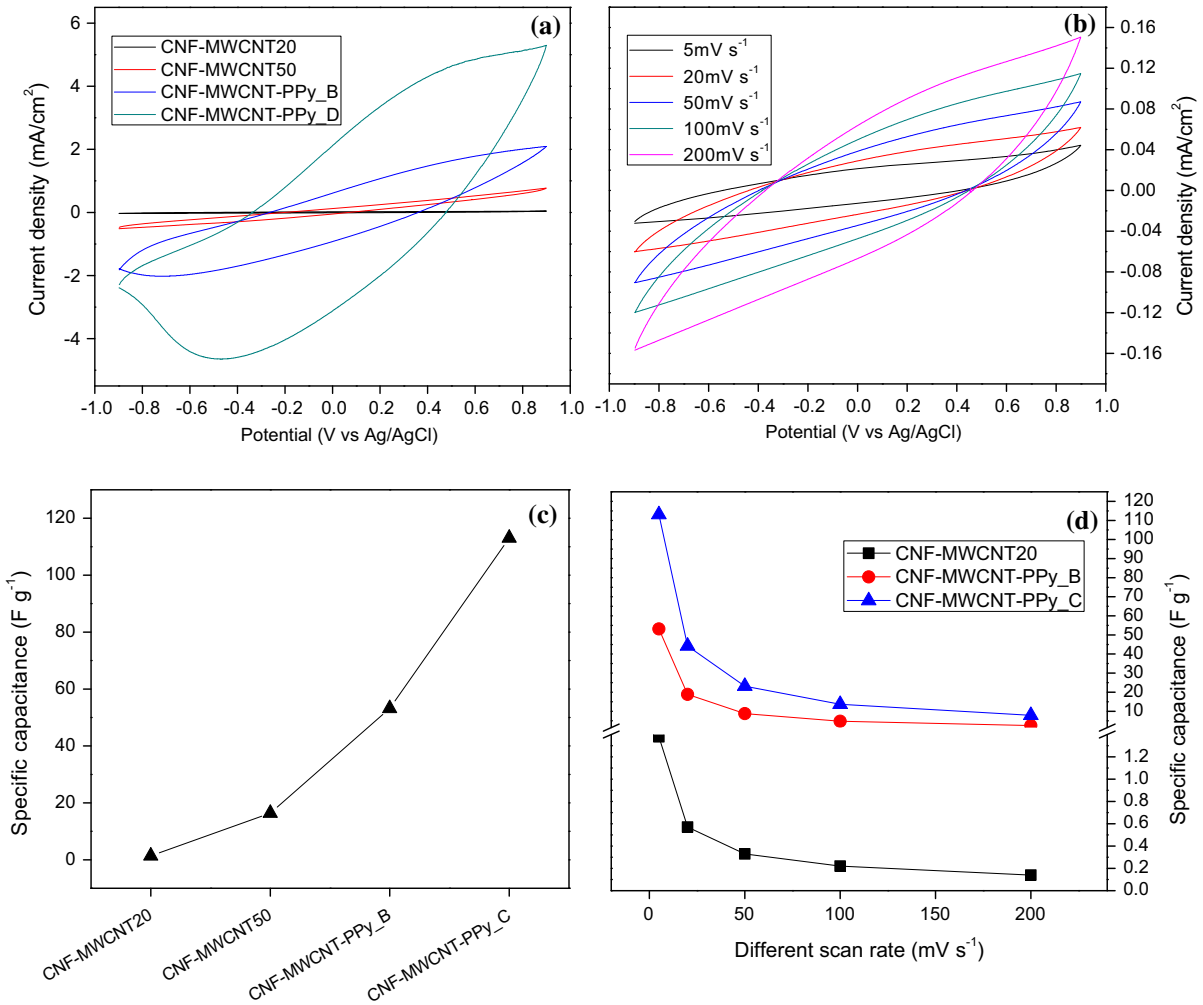

Fig. 6 Cyclic voltammograms of **a** binary and ternary nanopapers at 5 mv s^{-1} of scan rate **b** CNF-MWCNT20 at different scan rates, **c** specific capacitances of binary and ternary nanopapers at 5 mv s^{-1} of scan rate, and **d** specific capacitances at different scan rates

This high specific capacitance can be explained by the direct interaction between the delocalized electrons on polymer chains and the MWCNT. In addition, it is known that the functional groups (carboxylic, hydroxyl) formed during the acid treatment are known to act as redox active (Peng et al. 2007). This result is similar to previous findings where the specific capacitance of PPy deposited on MWCNT via electrochemical polymerization was 163 F g^{-1} (Frackowiak et al. 2001). It was mentioned that PPy has capability to provide the capacitive response via fast redox reactions of the conjugated area in polymer networks (Xiong et al. 2015). The coating of PPy on the outer surface of the nanotube enhance the faradaic charge transfer reaction providing a high specific capacitance (Fu et al. 2013; Yu et al. 2013).

Conclusions

The aim of the current study was to study the effect of multi-walled carbon nanotubes (MWCNTs) and polypyrrole (PPy) on the electrical properties of cellulose nanopapers. For this purpose, TEMPO-oxidized cellulose nanofibers (CNFs) were combined with multi-walled carbon nanotubes and PPy polymer to produce binary and ternary formulations of conductive nanopapers. Cellulose nanofibril network acted as strong and tough matrix, where the negatively charged TEMPO-oxidized cellulose nanofibers assisted the formation of nanostructured and nanodispersed CNF-MWCNT nanopapers. High mechanical properties and good conductive response was established for this binary formulation. The coating of PPy produced a ternary multiphase material with improved conductivity and electrochemical properties, by keeping the nanostructure of the multifunctional material. The ternary formulation produced nanopapers with an electrical conductivity of 2.41 S cm^{-1} and a specific capacitance of 113 F g^{-1}, much higher than those for the binary formulation with 50 wt% of MWCNT (0.78 S cm^{-1} and 16.4 F g^{-1}). Moreover, the experimental approach is a simple and environmentally friendly method based on mixing/sonication/filtering process. The production of ternary conductive nanopaper is still less expensive than the binary nanopaper because of the lower price of PPy compared to MWCNTs. These findings and the novel concept open the future application of cellulose nanofibers in the field of green and flexible electronics for a wide range of applications, such as electrochemical energy storage devices.

Acknowledgments The authors want to thank the financial support of the European Commission (Erasmus Mundus project Techno II, ref. 372228-1-2012-1-FR-ERA MUNDUS-EMA21).

REFERENCES

Adsul MG, Rey DA, Gokhale DV (2011) Combined strategy for the dispersion/dissolution of single walled carbon nanotubes and cellulose in water. J Phys Chem 21:2054–2056. doi:10.1039/c0jm03186k

Ahmed DS, Haider AJ, Mohammad MR (2013) Comparesion of functionalization of multi-walled carbon nanotubes treated by oil olive and nitric acid and their characterization. Energy Procedia 36:1111–1118. doi:10.1016/j.egypro.2013.07.126

Anderson RE, Guan J, Ricard M et al (2010) Multifunctional single-walled carbon nanotube–cellulose composite paper. J Mater Chem 20:2400–2407. doi:10.1039/b924260k

Baughman RH, Zakhidov AA, de Heer WA (2002) Carbon nanotubes—the route toward applications. Science 297:787–792. doi:10.1126/science.1060928

Chen BGZ, Shaffer MSP, Coleby D et al (2000) Carbon nanotube and polypyrrole composites: coating and doping. Adv Mater 12:522–526

Deng L, Young RJ, Kinloch IA et al (2013) Supercapacitance from cellulose and carbon nanotube nanocomposite fibers. ACS Appl Mater Interfaces 5:9983–9990. doi:10.1021/am403622v

Dufresne A (2012) Nanocellulose: potential reinforcement in composites. In: John MJ, Sabu T (eds) Natural polymers: volume 2: nanocomposites. Royal Society of Chemistry Publishing, Cambridge, UK, pp 1–32. ISBN:978-1-84973-403-5

Feng X (2015) Nanocarbons for advanced energy storage. Wiley-VCH, Weinheim

Frackowiak E, Jurewicz K, Delpeux S, Bertagna V (2001) Supercapacitors from nanotubes/polypyrrole composites. Chem Phys Lett 347:36–40

Fu H, Du Z, Zou W et al (2013) Carbon nanotube reinforced polypyrrole nanowire network as a high-performance supercapacitor electrode. J Mater Chem A 1:14943–14950. doi:10.1039/C3TA12844J

Fukuzumi H, Saito T, Iwata T et al (2009) Transparent and high gas barrier films of cellulose nanofibers prepared by TEMPO-mediated oxidation. Biomacromolecules 10:162–165. doi:10.1021/bm801065u

Gao K, Shao Z, Wang X et al (2013) Cellulose nanofibers/multi-walled carbon nanotube nanohybrid aerogel for all-solid-state flexible supercapacitors. RSC Adv 3:15058–15064. doi:10.1039/c3ra42050g

González I, Alcalà M, Chinga-Carrasco G et al (2014) From paper to nanopaper: Evolution of mechanical and physical properties. Cellulose 21:2599–2609. doi:10.1007/s10570-014-0341-0

Goyanes S, Rubiolo GR, Salazar A et al (2007) Carboxylation treatment of multiwalled carbon nanotubes monitored by

infrared and ultraviolet spectroscopies and scanning probe microscopy. Diam Relat Mater 16:412–417. doi:10.1016/j.diamond.2006.08.021

Hamedi MM, Hajian A, Fall AB et al (2014) Highly conducting, strong nanocomposites based on nanocellulose-assisted aqueous dispersions of single-wall carbon nanotubes. ACS Nano 8:2467–2476. doi:10.1021/nn4060368

Henriksson M, Fogelström L, Berglund LA et al (2011) Novel nanocomposite concept based on cross-linking of hyperbranched polymers in reactive cellulose nanopaper templates. Compos Sci Technol 71:13–17. doi:10.1016/j.compscitech.2010.09.006

Hermant MC (2009) Manipulating the percolation threshold of carbon nanotubes in polymeric comosites. Eindhoven University of Technology, Eindhoven. ISBN:978-90-386-1771-8

Hirsch A (2002) Functionalization of single-walled carbon nanotubes. Angew Chemie Int Ed 41:1853–1859. doi:10.1002/1521-3773(20020603)41:11<1853:AID-ANIE1853>3.0.CO;2-N

Hung NT, Anoshkin IV, Dementjev AP et al (2008) Functionalization and solubilization of thin multiwalled carbon nanotubes. Inorg Mater 44:219–223. doi:10.1134/S0020168508030023

Jung R, Kim HS, Kim Y et al (2007) Electrically conductive transparent paper using multiwalled carbon nanotubes. J Polym Sci Part B: Polym Phys 46:1235–1242. doi:10.1002/polb

Kargarzadeh H, Ahmad I, Abdullah I et al (2012) Effects of hydrolysis conditions on the morphology, crystallinity, and thermal stability of cellulose nanocrystals extracted from kenaf bast fibers. Cellulose 19:855–866. doi:10.1007/s10570-012-9684-6

Koga H, Saito T, Kitaoka T et al (2013) Transparent, conductive, and printable composites consisting of TEMPO-oxidized nanocellulose and carbon nanotube. Biomacromolecules 14:1160–1165. doi:10.1021/bm400075f

Lay M, Mendez JA, Delgado-Aguilar M et al (2016) Strong and electrically conductive nanopaper from cellulose nanofibers and polypyrrole. Carbohydr Polym 152:361–369. doi:10.1016/j.carbpol.2016.06.102

Li X, Zhitomirsky I (2013) Electrodeposition of polypyrrole-carbon nanotube composites for electrochemical supercapacitors. J Power Sources 221:49–56. doi:10.1016/j.jpowsour.2012.08.017

Lu P, Hsieh Y-L (2010) Multiwalled carbon nanotube (MWCNT) reinforced cellulose fibers by electrospinning. ACS Appl Mater Interfaces 2:2413–2420. doi:10.1021/am1004128

Nyholm L, Nyström G, Mihranyan A, Strømme M (2011) Toward flexible polymer and paper-based energy storage devices. Adv Mater 23:3751–3769. doi:10.1002/adma.201004134

Nyström G, Strømme M, Sjödin M, Nyholm L (2012) Rapid potential step charging of paper-based polypyrrole energy storage devices. Electrochim Acta 70:91–97. doi:10.1016/j.electacta.2012.03.060

Pandey JK, Takagi H, Kakagaito AN, Kim H (eds) (2015) Handbook of polymer nanocomposites. Processing, performance and application, 1st edn. Springer, New York

Peng C, Jin J, Chen GZ (2007) A comparative study on electrochemical co-deposition and capacitance of composite films of conducting polymers and carbon nanotubes. Electrochim Acta 53:525–537. doi:10.1016/j.electacta.2007.07.004

Peng C, Zhang S, Jewell D, Chen GZ (2008) Carbon nanotube and conducting polymer composites for supercapacitors. Prog Nat Sci 18:777–788. doi:10.1016/j.pnsc.2008.03.002

Saito T, Kimura S, Nishiyama Y, Isogai A (2007) Cellulose nanofibers prepared by TEMPO-mediated oxidation of native cellulose. Biomacromolecules 8:2485–2491. doi:10.1021/bm0703970

Salajkova M, Valentini L, Zhou Q, Berglund LA (2013) Tough nanopaper structures based on cellulose nanofibers and carbon nanotubes. Compos Sci Technol 87:103–110

Saville P (2005) Polypyrrole, formation and use. Defence R&D Canada-Atlantic. Technical Memorandum. DRDC Atlantic TM 2005-004, pp 1–51

Sehaqui H, Zhou Q, Ikkala O, Berglund LA (2011) Strong and tough cellulose nanopaper with high specific surface area and porosity. Biomacromolecules 12:3638–3644

Soni B, Hassan EB, Mahmoud B (2015) Chemical isolation and characterization of different cellulose nanofibers from cotton stalks. Carbohydr Polym 134:581–589. doi:10.1016/j.carbpol.2015.08.031

Wang M, Anoshkin IV, Nasibulin AG et al (2013) Modifying native nanocellulose aerogels with carbon nanotubes for mechanoresponsive conductivity and pressure sensing. Adv Mater 25:2428–2432. doi:10.1002/adma.201300256

Xiong P, Zhu J, Wang X (2015) Recent advances on multicomponent hybrid nanostructures for electrochemical capacitors. J Power Sources 294:31–50. doi:10.1016/j.jpowsour.2015.06.062

Yan Huang Y, Terentjev ME (2012) Dispersion of carbon nanotubes: mixing, sonication, stabilization, and composite properties. Polymers (Basel) 4:275–295. doi:10.3390/polym4010275

Yang BH (2011) Investigation and characterization of oxidized cellulose and cellulose nanofiber films. McGill University, Montreal

Yang C, Chen C, Pan Y et al (2015) Flexible highly specific capacitance aerogel electrodes based on cellulose nanofibers, carbon nanotubes and polyaniline. Electrochim Acta 182:264–271. doi:10.1016/j.electacta.2015.09.096

Yu R, Chen L, Liu Q et al (1998) Platinum deposition on carbon nanotubes via chemical modifica tion. Am Chem Soc 10:718–722

Yu G, Xie X, Pan L et al (2013) Hybrid nanostructured materials for high-performance electrochemical capacitors. Nano Energy 2:213–234. doi:10.1016/j.nanoen.2012.10.006

Zhang H, Cao G, Yang Y (2009) Carbon nanotube arrays and their composites for electrochemical capacitors and lithium-ion batteries. Energy Environ Sci 2:932–943. doi:10.1039/b906812k